ORIGINAL ARTICLE

Journal of Cachexia, Sarcopenia and Muscle 2018; **9**: 1003–1017
Published online 2 August 2018 in Wiley Online Library (wileyonlinelibrary.com) **DOI:** 10.1002/jcsm.12339

Oxidative stress-induced dysregulation of excitation–contraction coupling contributes to muscle weakness

Rizwan Qaisar[1], Shylesh Bhaskaran[1], Pavithra Premkumar[1], Rojina Ranjit[1], Kavithalakshmi Satara Natarajan[1], Bumsoo Ahn[1], Kaitlyn Riddle[1], Dennis R. Claflin[2,3], Arlan Richardson[5,3,6], Susan V. Brooks[4] & Holly Van Remmen[1,5]*

[1]*Aging and Metabolism Research Program, Oklahoma Medical Research Foundation, Oklahoma City, OK, USA,* [2]*Department of Surgery, Section of Plastic Surgery, University of Michigan, Ann Arbor, MI, USA,* [3]*Department of Biomedical Engineering, University of Michigan, Ann Arbor, MI, USA,* [4]*Department of Molecular and Integrative Physiology, University of Michigan, Ann Arbor, MI, USA,* [5]*Oklahoma City VA Medical Center, Oklahoma City, OK, USA,* [6]*Department of Geriatric Medicine and the Reynolds Oklahoma Center of Aging, Oklahoma University Health Science Center, Oklahoma City, OK, USA*

Abstract

Background We have previously shown that the deletion of the superoxide scavenger, CuZn superoxide dismutase, in mice (*Sod1*$^{-/-}$ mice) results in increased oxidative stress and an accelerated loss of skeletal muscle mass and force that mirror the changes seen in old control mice. The goal of this study is to define the effect of oxidative stress and ageing on muscle weakness and the Excitation Contraction (EC) coupling machinery in age-matched adult (8–10 months) wild-type (WT) and *Sod1*$^{-/-}$ mice in comparison with old (25–28 months) WT mice.

Methods *In vitro* contractile assays were used to measure muscle contractile parameters. The activity of the sarcoplasmic reticulum Ca^{2+} ATPase (SERCA) pump was measured using an NADH-linked enzyme assay. Immunoblotting and immunofluorescence techniques were used to measure protein expression, and real-time reverse transcription PCR was used to measure gene expression.

Results The specific force generated by the extensor digitorum longus muscle was reduced in the *Sod1*$^{-/-}$ and old WT mice compared with young WT mice along with significant prolongation of time to peak force, increased half relaxation time, and disruption of intracellular calcium handling. The maximal activity of the SERCA calcium uptake pump was significantly reduced in gastrocnemius muscle from both old WT (≈14%) and adult *Sod1*$^{-/-}$ (≈33%) mice compared with young WT mice along with increased expression of sarcolipin, a known inhibitor of SERCA activity. Protein levels of the voltage sensor and calcium uptake channel proteins dihydropyridine receptor α1 and SERCA2 were significantly elevated (≈45% and ≈57%, respectively), while the ratio of calstabin, a channel stabilizing protein, to ryanodine receptor was significantly reduced (≈21%) in *Sod1*$^{-/-}$ mice compared with young WT mice. The changes in calcium handling were accompanied by substantially elevated levels of global protein carbonylation and lipid peroxidation.

Conclusions Our data suggest that the muscle weakness in *Sod1*$^{-/-}$ and old WT mice is in part driven by reactive oxygen species-mediated EC uncoupling and supports a role for reduced SERCA pump activity in compromised muscle function. The novel quantitative mechanistic data provided here can lead to potential therapeutic interventions of SERCA dysfunction for sarcopenia and muscle diseases.

Keywords Excitation contraction coupling; Skeletal muscle; SERCA pump; Sarcolipin; Sod1; Sarcopenia

Received: 14 March 2018; Accepted: 25 June 2018
**Correspondence to: Holly Van Remmen, PhD, Aging and Metabolism Research Program, Oklahoma Medical Research Foundation, 825 NE 13th Street, Oklahoma City, OK 73104, USA. Phone: 405-271-2520. Fax: 271-3470, Email: holly-vanremmen@omrf.org*

Introduction

Sarcopenia, the age-related loss of muscle mass and strength,[1] is a major cause of morbidity and mortality in the elderly population. While muscle atrophy contributes to weakness, the decline in muscle strength is more rapid than the atrophy, suggesting a deficit in intrinsic force-generating properties of the muscle.[2] The age-related muscle weakness independent of loss of mass is defined as dynapenia[3] and involves the excitation–contraction coupling machinery of the muscle fibres.[4] A progressive increase in cellular oxidative stress during ageing has been implicated as a major contributor to sarcopenia. Accordingly, we have previously reported a direct correlation between muscle reactive oxygen species and the muscle mass during normal ageing and in muscle diseases.[5]

Excitation–contraction coupling involves a sequence of events whereby action potential-driven excitation of the sarcolemma results in rapid changes in cytoplasmic calcium concentration leading to activation of force-generating machinery in the sarcomere.[6] The electromechanical conduction requires activation of dihydropyridine receptors (DHPRs) in the sarcolemma and the subsequent release of calcium into the sarcoplasm from the intracellular calcium stores [sarcoplasmic reticulum (SR)] through the Ca^{2+} release channels [ryanodine receptors (RyRs)]. The Ca^{2+} binds to regulatory proteins in the sarcomere initiating the contraction. Muscle relaxation occurs when Ca^{2+} is transported back from the sarcoplasm into the SR by the SR Ca^{2+} ATPase (SERCA) pumps. In mammalian skeletal muscle, this process may dictate the rates of relaxation and a termination of a variety of Ca^{2+}-dependent signalling pathways and gene transcription events that influence muscle quality and quantity.[7] Post-translational modifications of calcium release channels (RyRs)[8] and SERCA pumps[9] in the SR membrane can perturb the Ca^{2+} regulation leading to an uncoupling of excitation and contraction. These processes imply the critical importance of calcium handling in the muscle fibre as dysregulation of calcium homoeostasis has been associated with reduced specific force in ageing[10,11] and conditions of increased oxidative stress.[12,13]

Our lab has previously used a mouse model of oxidative stress that was created by deleting cellular antioxidant enzyme Cu/Zn superoxide dismutase resulting in many features of rapid and accelerated sarcopenia.[14–16] The reduction in specific force in these mice is only partially rescued via direct muscle stimulation that bypasses the neuromuscular junction, suggesting a loss of functional innervation in these mice[15] but also defects within fibres. Moreover, interrogation of the function of single permeabilized fibres showed no difference between *Sod1*$^{-/-}$ and wild-type (WT) mice indicating no impairment in the *Sod1*$^{-/-}$ mice in the inherent function of the contractile machinery[17] and suggests that there may be declines in the functioning of the excitation contraction machinery in CuZn superoxide dismutase (CuZnSOD) deficient muscle fibres. An association between functional denervation and excitation contraction uncoupling is well established in animal models and humans[18–20] and is partly explained by reduced quality and/or quantity of SR proteins. The mice lacking *Sod1* show increased oxidative damage to DNA, proteins and lipids in skeletal muscle, and other tissues that is associated with muscle atrophy and functional decline. More specifically, these muscles show increased 3-nitrotyrosine content,[21] which is known to disturb SR protein function and the muscle contractile force.[22]

The goal of this study was to determine whether the loss of innervation and the chronic increase in cellular oxidative stress in the *Sod1*$^{-/-}$ mice affect the excitation–contraction apparatus in a manner similar to muscles of old WT mice. To achieve this purpose, we measured SERCA activity and *in vitro* muscle contractile function. We also looked at the expression of key proteins involved in calcium handling. Further, as possible contributors to the muscle weakness, we also determined the quality and quantity of proteins involved in force generation. We hypothesize that, in skeletal muscles of *Sod1*$^{-/-}$ mice, EC coupling is impaired contributing to the sarcopenia phenotype.

Material and methods

Animals

The generation of *Sod1*$^{-/-}$ mice is described in detail elsewhere.[18,23] Male C57BL/6J mice were maintained under specific pathogen free conditions, housed 3–4/cage, maintained in a 12:12 (light: dark) cycle, and provided with food and water *ad libitum*. Age of the mice at the time of sacrifice was 8–10 months for young WT and *Sod1*$^{-/-}$ mice and 25–28 months for old WT mice (n = 10–12 mice/group). At sacrifice, mice were euthanized via CO_2 inhalation, and tissues were immediately excised and weighed. All tissues except those used for immunostaining and contractile recordings were snap frozen and stored at −80°C. All animal protocols were consistent with The Guide for the Care and Use of Laboratory Animals and approved by the institutional Animal Care and Use Committee at the Oklahoma Medical Research Foundation (OKC, OK, USA).

Protein preparation and western blot

Muscles were ground in a mortar and pestle under liquid nitrogen, and frozen muscle powder was placed into Radioimmunoprecipitation assay (RIPA) buffer containing 50 mM Tris (pH 7.4), 150 mM NaCl, and protease inhibitors. Samples were homogenized on ice and centrifuged at 10 000 g for 10 min at 4°C. Protein content of samples was

determined using the bicinchoninic acid method (Sigma-Aldrich, Poole, UK). For assessment of specific proteins in muscle, 20 mg of total protein was applied to a 4–20% mini-PROTEAN TGX precast gel with a 4% stacking gel (Bio-Rad Laboratories Ltd, Hemel Hempstead, UK). The separated proteins were transferred onto nitrocellulose membranes by western blotting. Membranes were probed using antibodies against calstabin, serca1, calsequestrin (Abcam, Cambridge, UK), DHPR, RYR (Thermo Scientific, USA), calcineurin, nuclear factor of activated T-cells (NFAT), calpain (Cell Signaling, Hitchin, UK), and CuZnSod (Enzo, Farmingdale, NY, USA). Horseradish peroxidase conjugated anti-rabbit IgG or anti-mouse IgG (Cell Signaling) was used as secondary antibody. Peroxidase activity was detected using an ECL Plus substrate (Amersham International Cardiff, UK), and band intensities were analysed using Quantity One Software (Bio-Rad Laboratories Ltd). All protein contents were normalized to protein levels determined by the ponceau stain.

Analysis of F_2-isoprostanes

Levels of F_2-isoprostanes in quadriceps muscle were measured as described previously.[24] Hind limb muscle is routinely studied for changes during ageing due to the increased response in this compartment. Quadriceps muscles were specifically chosen for this assay due to the amount of muscle tissue required for this assay (200 mg). Briefly, 200 mg of tissue was homogenized in 10 mL of ice-cold Folch solution (CHCl3: MeOH, 2:1) containing butylated hydroxytoluene. The mixture was incubated at room temperature for 30 min. Two millilitres of 0.9% NaCl was added and mixed well. The homogenate was centrifuged at 3000 g for 5 min at 4°C. The aqueous layer was discarded, while the organic layer was secured and evaporated to dryness under N2 at 37°C. Esterified F_2-isoprostanes were measured using gas chromatography–mass spectrometry. The level of F_2-isoprostanes in muscle tissues was expressed as nanograms of 8-Iso-$PGF_{2\alpha}$, per gram of muscle tissue.

Real-time PCR

Total RNA was extracted from the gastrocnemius muscles of the young and old WT and *Sod1*$^{-/-}$ mice using TRI reagent (Life Technologies, Grand Island, NY, USA). RNA purity and yield were determined by measuring the absorbance at 260 and 280 nm. cDNA was prepared from 1 mg of the total RNA using iScriptTM cDNA Synthesis kit (Bio-Rad, Hercules, CA, USA); 2.5 ng of cDNA samples were amplified using primers for DHPR1α, Calstabin, Calsequestrin, SERCA1, SERCA2, Sarcolipin, and 18S along with fast SYBR green master mix (Applied Biosystems, Grand Island, NY, USA). The data were analysed using the $\Delta\Delta$Ct method.

Contractile measurements

Contractility measurements were performed on isolated extensor digitorum longus (EDL) muscle using a 1200A *in vitro* test system (Aurora Scientific Inc., Aurora, ON, Canada). The hind limb EDL muscle was chosen for analysis due to the well-documented response of this muscle to oxidative stress related to ageing and other muscle diseases. Muscles were individually tied to a model 300C servomotor (Aurora Scientific Inc.) and fixed within a water bath containing an oxygenated (95% O_2, 5% CO_2) Krebs-Ringer solution (in mM: 137 NaCl, 5 KCl, 1 $MgSO_4$, 1 NaH_2PO_4, 24 $NaHCO_3$, and 2 $CaCl_2$) maintained at 32°C. Computer controlled stimulation was applied through a model 701C stimulator (Aurora Scientific Inc.) via flanking platinum plate field stimulus electrodes at supramaximal voltage, 0.2 ms pulse width, and at optimum length for twitch force production (i.e. L_o). The times required to reach maximal force from baseline [time to peak (TTP)] and to achieve 50% relaxation from the peak [half relaxation time ($RT_{1/2}$)] were measured for twitch and tetanic contractions. Force frequency curves were generated with stimulation frequencies between 1 and 300 Hz, while the fatigue protocol consisted of repeated 300 ms trains of 150 Hz stimuli, every 5 s for a total of 400 s. All data were recorded and analysed using commercial software (DMC and DMA, Aurora Scientific Inc.). Specific force (N/cm^2) was measured using muscle length and weight as described elsewhere.[25]

The methods and instrumentation use to measure the contractility of the lumbrical muscles were very similar to those used to measure EDL contractility and have been described in detail previously.[26] Notable differences were that force-frequency and fatigue responses were not determined for the lumbrical muscles, and experiments were performed in a custom-built chamber with a quartz floor to allow excitation of the fura-2 and mag-fura-2 fluorescent dyes with ultraviolet light. Experimental temperature was 25°C, and acquisition and analysis were performed using custom software developed in LabVIEW (National Instruments, Austin, TX). Because the lumbrical muscle is too small to weight accurately, cross-sectional area was estimated by measuring maximum muscle diameters using a calibrated reticule in the microscope eyepiece and assuming a circular cross section.[26]

Sarcoplasmic reticulum Ca^{2+} ATPase activity

The measurement of SERCA ATPase activity was performed at 37°C using a spectrophotometric assay as described elsewhere.[27] The gastrocnemius muscle, which has been shown to be particularly responsive to age and oxidative stress-related changes in mass and force generation, was used for this analysis. Briefly, muscle samples (15–20 mg) were diluted 1:10 (wt/vol) and manually homogenized in

ice-cold homogenizing buffer (pH 7.5) containing (in mM) 250 sucrose, 5 HEPES, 0.2 PMSF, and 0.2% sodium azide (NaN_3). Ca^{2+}-dependent Ca^{2+}-ATPase activity was measured in the assay buffer containing 100 mM KCl, 20 mM HEPES, pH 7.0, 10 mM $MgCl_2$, 10 mM NaN3, 10 mM phospho*enol*pyruvate, 1 mM EGTA, 5 mM ATP, 18 U/mL of both lactate dehydrogenase and pyruvate kinase, and 1 mM Ca^{2+} ionophore A-23187 (C-7522, Sigma). The reaction mixture was divided into 10 aliquots of 300 μL and mixed with $CaCl_2$ to generate 10 different Ca^{2+}concentrations, ranging between 7.6 and 5 *p*Ca units. The reaction was started by adding 0.3 mM NADH. Basal activity was determined in the presence of 40 μM of the Ca^{2+}-ATPase inhibitor cyclopiazonic acid (C-1530, Sigma) in dimethyl sulfoxide.

Calpain activity

Because SERCA dysfunction can perturb cytosolic calcium levels leading to activation of calcium-dependent proteases, we measured the calpain activity in the gastrocnemius muscle homogenates as previously described[28] with slight modifications. Briefly, 100 μg of protein was added to a buffer containing 50 mM HEPES, 100 mM NaCl, 0.1% CHAPS, 10 mM DTT, 1 mM EDTA, 10% glycerol, pH: 7.4, and a fluorogenic substrate (Suc-LLVY-AMC) cleaved by calpain. Immediately after addition of the substrate, a baseline fluorescent measurement was performed using a spectrofluorometer (excitation frequency: 355 nm, emission frequency: 460 nm). The measurement was repeated after 60 min of incubation at 37°C. AMC standard were used to create a calibration curve, and activity was quantified as nanomoles of AMC generated per minute per milligram of tissue homogenate protein. The difference between AMC generation from incubation of homogenates with Suc-LLVY-AMC in the presence and absence of calpain inhibitor III was taken as an index of calpain activity.

Intracellular calcium in whole muscles

Intracellular calcium levels were monitored in lumbrical muscles from WT and *Sod1*$^{-/-}$ mice (age 8–10 months) using calcium-sensitive fluorescent dyes loaded by incubation in their acetoxymethyl (AM) ester form. Pluronic F-127 (0.01% *w*/*v*; Thermo Fisher) was used as a dispersing agent. The simple architecture (essentially a parallel fibres arrangement) and small size of lumbrical muscles facilitated loading of fluorescence dyes and exchange of gases and metabolites across minimal diffusion distance. Calcium levels were recorded under three conditions: at rest, following a 5 s maximum tetanic contraction, and in response to twitch stimuli. Experiments to determine resting and post-tetanic calcium levels were performed in the same series of lumbrical muscles by loading the highly sensitive calcium indicators fura-2 AM (16.4 μM) and fluo-4 AM (15 μM) simultaneously for 30 min at 25°C. To determine resting levels, fura-2 fluorescence was excited at 340 and 375 nm (bandwidth 1.25 nm). The excitation source was a 75 W xenon lamp, and wavelengths were selected using a diffraction grating monochromator (PTI, model Delta RAM). Fluorescence responses were passed through a 510 nm emission filter (bandwidth 40 nm) before being quantified using a photomultiplier tube (Hamamatsu model R1527) in photon counting mode. After subtracting corresponding pre-loading backgrounds, the ratio of the fura-2 fluorescence intensities (340/375) was formed and taken as an indication of the resting calcium level.

In the presence of contractile activity, fura-2 becomes less reliable as a calcium indicator because its excitation and emission spectra overlap those of NAD(P)H.[29–31] The time course of the return of calcium to resting level following a long tetanic contraction was therefore monitored by recording the fluorescence response of fluo-4, which is not contaminated by contraction-induced NAD(P)H fluctuations. Fluo-4 fluorescence was excited at 493 nm (bandwidth 1.25 nm) and passed through a 535 nm emission filter (bandwidth 40 nm) to a photomultiplier tube in photon-counting mode, sampling at 100 s^{-1}. A line was fitted to the fluo-4 response beginning 60 s before the 5 s tetanic contraction and ending 420 s after the initiation of contraction, but excluding a 180 s segment that began with the contraction. Thus, the fitted line served to establish the decline in fluo-4 fluorescence over time due to dye leakage, extrusion, bleaching, etc. The raw fluo-4 response was divided by the fitted line to produce a 'detrended' response, which was then shifted such that the average value of the 60 s pre-stimulus recording (i.e. the resting level) was zero. The time required for the modified fluo-4 response to decay to within 50% and 25% of the resting level was measured relative to the level reached 1.5 s after cessation of tetanic stimulation. The 1.5 s post-contraction delay was incorporated to allow time for the calcium concentration and its rate of change to reach levels that could be reported by fluo-4 with minimal distortion.[32]

Experiments to determine the dynamic calcium responses to twitch stimuli were performed on a separate series of lumbrical muscles by loading the low-affinity calcium indicator mag-fura-2 AM (10 μM) for 30 min at 25°C. Mag-fura-2 fluorescence was excited at 344 and 375 nm (bandwidth 10 nm), and responses were passed through a 510 nm emission filter (bandwidth 40 nm) before entering a photomultiplier tube operating in analogue mode, which results in higher time-resolution and reduced noise when compared with photon counting. The experimental sequence consisted of first recording twitch force and mag-fura-2 fluorescence during excitation at 344 nm, waiting 20 s, and then recording twitch force and mag-fura-2 fluorescence during excitation at 375 nm. The alternating sequence was

repeated until a total of 16 responses had been recorded at each excitation wavelength. Pre-loading backgrounds were then subtracted from all fluorescence records, and the 16 responses at each excitation wavelength were averaged. Finally, the ratio of the averaged mag-fura-2 fluorescence intensities was formed (344/375) and taken as an undistorted representation of the rapid intracellular changes in calcium concentration that give rise to a twitch contraction.[33] All fluorescent dyes were obtained from Thermo Fisher. Additional details on the techniques and apparatus used to measure lumbrical muscle contractile properties and fluorescence have been described previously.[26]

Protein carbonylation

Protein oxidation in tissues was determined by the level of protein carbonyls using a modification of the original method described by Ahn *et al*.[34] Gastrocnemius muscles were utilized due to large body of literature on the response of these muscles to age and *Sod1* deficiency. In brief, fresh tissue was homogenized in degassed 20 mM sodium phosphate buffer, pH 6.0, containing 0.5 mM $MgCl_2$, 1 mM EDTA, and protease cocktail inhibitors (500 μM AEBSF, HCl, 150 nM aprotinin, 0.5 mM EDTA, disodium salt, and 1 μM leupeptin hemisulfate). For the cytoplasmic fraction, the homogenate was centrifuged at 100 000 g at 4°C for 1 h, and the supernatant was saved for further processing. One per cent streptomycin sulfate was added to remove nucleic acids. The protein samples were then bubbled with nitrogen for 15 s at 25 kPa followed by treatment with 0.3 M guanidine HCl for partial unfolding of the proteins in the sample. The hydrazine reagent, fluorescein-5-thiosemicarbazide (FTC, Molecular Probes, Eugene, OR, USA) (1 mM), was added and incubated for 2 h at 37°C in the dark. The excess unreacted FTC was removed by precipitation with an equal volume of 20% tricholoroacetic acid followed by washing 4 times with ethanol/ethyl acetate (1/1) (*v*/v). Equal amounts of protein were loaded on a 12% sodium dodecyl sulfate polyacrylamide gel electrophoresis to resolve the FTC-labelled proteins. A fluorescence scan of the gel was used to measure the amount of bound FTC, i.e. the amount of protein carbonyls. The gel was stained with Coomassie blue, and the protein concentration was determined. The carbonyl content of the protein samples was expressed as the ratio of FTC fluorescence (carbonyls) to Coomassie blue absorption (protein concentration).

Myosin heavy chains quantification and myosin heavy chain isoform composition

Gastrocnemius muscles were homogenized in high salt lysis buffer consisting of 0300 mM NaCl, 0.1 M NaH_3PO_4, 0.05 M Na_2PO_4, 0.01 M Na_4P2O_7, 1 mM $MgCl_2$, 10 mM EDTA, and 1 mM DTT (pH 6.5) and protease inhibitors. Tissue lysates were subsequently centrifuged at 16 000 g for 3 min at 4°C. Supernatant was collected, and 0.6 μg protein was loaded/lane into a 10% sodium dodecyl sulfate polyacrylamide gel electrophoresis and run at 200 V for 50 min at 4°C. The gel was stained with Coomassie blue, and the optical densities of the bands corresponding to myosin heavy chain (MHC) and actin were quantified.

For MHC isoforms composition, cryosections of gastrocnemius muscles were stained with monoclonal anti-MHC antibodies as described elsewhere.[35] All images were taken with Nikon Eclipse Ni confocal microscope and analysed with Nikon Elements C image acquisition software.

Statistical analysis

Data are presented as mean ± SEM, and the comparisons among the three groups were performed by one-way analysis of variance. Data were analysed using Sigma plot 12, and *P* values of less than 0.05 were considered statistically significant.

Results

The absence of CuZnSOD protein was confirmed in the gastrocnemius muscles of the *Sod1*$^{-/-}$ mice (*Figure* 1). This is previously reported to have no effect on the other major antioxidant enzymes in the muscle fibre.[36]

Body weights and muscle weights

The adult *Sod1*$^{-/-}$ mice show significantly smaller body mass ($P < 0.001$) than age matched young WT and the old WT mice (*Figure* 1A). The gastrocnemius muscles from the old WT and *Sod1*$^{-/-}$ mice showed reduced mass when compared with young WT mice, which remained reduced when normalized to body weight. The absolute muscle weights of the quadriceps, tibialis anterior (TA), and EDL were significantly reduced in the old WT and *Sod1*$^{-/-}$ mice as compared with young WT mice. However, these differences were limited to old WT mice when normalized to body weights (*Table* S1).

Contractile function

We have previously shown that the gastrocnemius muscle of the *Sod1*$^{-/-}$ mice shows significant weakness in comparison with the age-matched controls,[37] which is due in part to disruption of neuromuscular junctions.[36,38,39] Here, we measured the *in vitro* contractile properties of EDL and lumbrical

Figure 1 Characteristics of mice used in the study. (A) Mouse age, body mass, and gastrocnemius muscle weights and (B) western blot analysis of CuZnSod1 expression in the gastrocnemius muscles from the young and old wild-type and *Sod1*$^{-/-}$ mice. Values are expressed as mean ± SEM (n = 8–12 per group); one-way analysis of variance. $^{*}P \leq 0.05$, $^{***}P \leq 0.001$, $^{****}P \leq 0.0001$. CuZnSOD, CuZn superoxide dismutase.

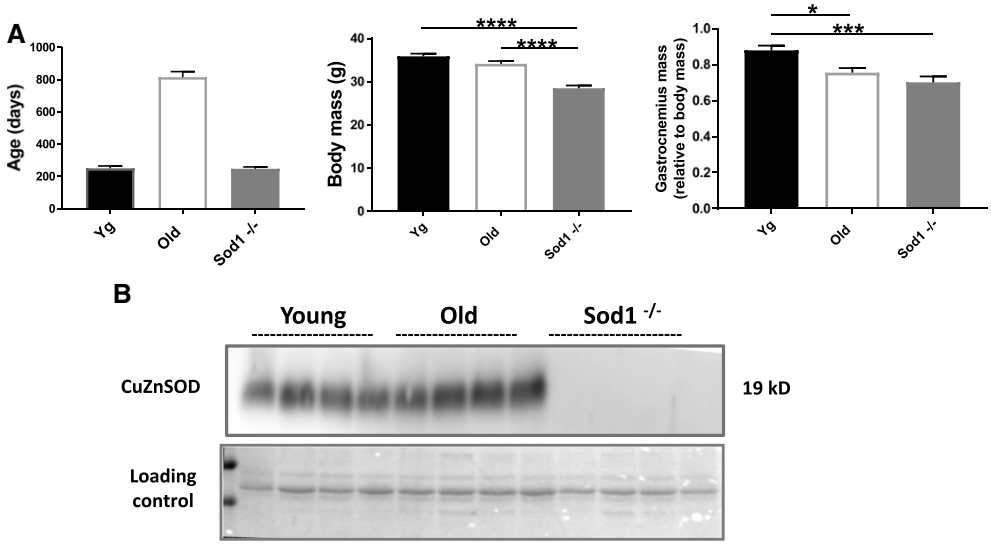

muscles focusing on the parameters of calcium regulation. In agreement with our previously reported findings, we found a significant decline in specific force in the EDL muscles of old WT mice (≈26%, $P < 0.05$) and *Sod1*$^{-/-}$ mice (≈24%, $P < 0.05$) when compared with young WT mice (*Table* 1). The twitch TTP and the $RT_{1/2}$ were not significantly different in the EDL muscles from old WT mice and *Sod1*$^{-/-}$ mice when compared with young WT mice. However, we report a significant prolongation of TTP and the $RT_{1/2}$ in the lumbrical muscles of *Sod1*$^{-/-}$ mice when compared with young WT mice (*Table* 1). Further, we assessed the calcium homoeostasis and the fibre-type profile by measuring the tetanic forces during a series of stimulus trains of increasing frequency. A significant downward shift in the force frequency curve between 100 and 300 Hz was observed in old WT and *Sod1*$^{-/-}$ mice EDL (*Figure* 2A). Fused tetanus was achieved at a lower stimulation frequency resulting in a leftward shift of the frequency for curve for muscles of old WT mice.

Table 1 Muscles contractile properties

	Young WT	Old WT	*Sod1*$^{-/-}$
EDL			
Absolute force (mN)	388.6 ± 15.3	301.4 ± 13.7*	309.4 ± 18.8*
Specific force (N/cm^2)	24.4 ± 0.41	18.0 ± 0.75*	18.8 ± 0.49*
TTP (ms)	17.38 ± 3.11	18 ± 3.29	18.35 ± 3.2
$RT_{1/2}$(ms)	30.35 ± 2.06	25 ± 1.86	26.15 ± 3.73
Lumbricals			
CSA (mm^2)	0.335 ± 0.017		0.277 ± 0.018*
Pt (mN)	21.8 ± 0.9		18.4 ± 0.8**
TTP (ms)	21.1 ± 0.3		22.6 ± 0.5*
$RT_{1/2}$(ms)	32.7 ± 0.8		38.6 ± 1.2**
Pt /Fo	0.429 ± 0.009		0.451 ± 0.01
Fo (mN)	50.8 ± 1.8		40.7 ± 1.4**
sFo (N/cm^2)	15.7 ± 1		15 ± 0.6

Contractile properties from extensor digitorum longus (EDL) and lumbricals muscles of young and old wild-type (WT) and *Sod1*$^{-/-}$ mice. CSA, cross-sectional area; Fo, absolute tetanic force; Pt, absolute twitch force; $RT_{½}$, twitch half relaxation time; sFo, specific force; TTP, time to peak twitch force. Values are expressed as mean ± SEM (n = 8–15 per group); one-way analysis of variance. *$P \leq 0.05$ vs. young WT. **$P \leq 0.01$ vs. young WT.

Intracellular calcium transients

Performance of cellular calcium release and sequestration functions were also assessed under more physiological conditions in intact lumbrical muscles (*Figure* 2B and 2C). The large, rapid calcium transients associated with twitch contractions were reduced in amplitude and took longer to decay in *Sod1*$^{-/-}$ compared with WT mice (*Figure* 3A). No difference was detected between lumbrical muscles from *Sod1*$^{-/-}$ and WT mice in either the resting calcium level or the slow return to resting level following a long tetanic contraction (*Figure* 3B).

Sarcoplasmic reticulum Ca^{2+} ATPase activity and regulator proteins

Reduced activity of SERCA has previously been reported in skeletal muscle during ageing and conditions of increased oxidative stress.[40,41] We hypothesized that the *Sod1*$^{-/-}$ mice

Figure 2 Muscle contractile properties. Muscle contractile properties measured in the young and old wild-type (WT) and *Sod1*$^{-/-}$ mice. (A) Force-frequency curves for extensor digitorum longus muscles represented as percentage of maximum force and specific force; (B) representative force (blue trace) and fluo-4 fluorescence (red trace) responses to 5 s maximum tetanic stimulation. Arrows indicate times of initiation and termination of stimulation. Upon termination of stimulation, force immediately returned to resting level, whereas the fluo-4 fluorescence remained elevated for several seconds. Relative to the level reached 1.5 s after stimulation was stopped, the times required for the fluo-4 response to decay to 50% ($t_{50\%}$) and 25% ($t_{25\%}$) were 6.4 and 15.7 s, respectively. Fluo-4 fluorescence units are $\Delta F/F_r$, where ΔF is fluorescence measured relative to resting level, and resting level is designated F_r. (C) Representative force (blue trace) and mag-fura-2 fluorescence (red trace) responses to twitch stimulation. Arrow indicates time at which a single stimulation pulse was delivered. The mag-fura-2 response was obtained by averaging 16 individual responses to excitation at 344 nm and 16 responses to excitation at 375 nm and then forming the ratio of the two averages (344/375). The force response is the average of all 32 recordings. Values are expressed as mean ± SEM (n = 8–12 per group); one-way analysis of variance. $^{*}P \leq 0.05$, $^{**}P \leq 0.01$, $^{***}P \leq 0.001$, $^{****}P \leq 0.0001$. AUC, area under the curve.

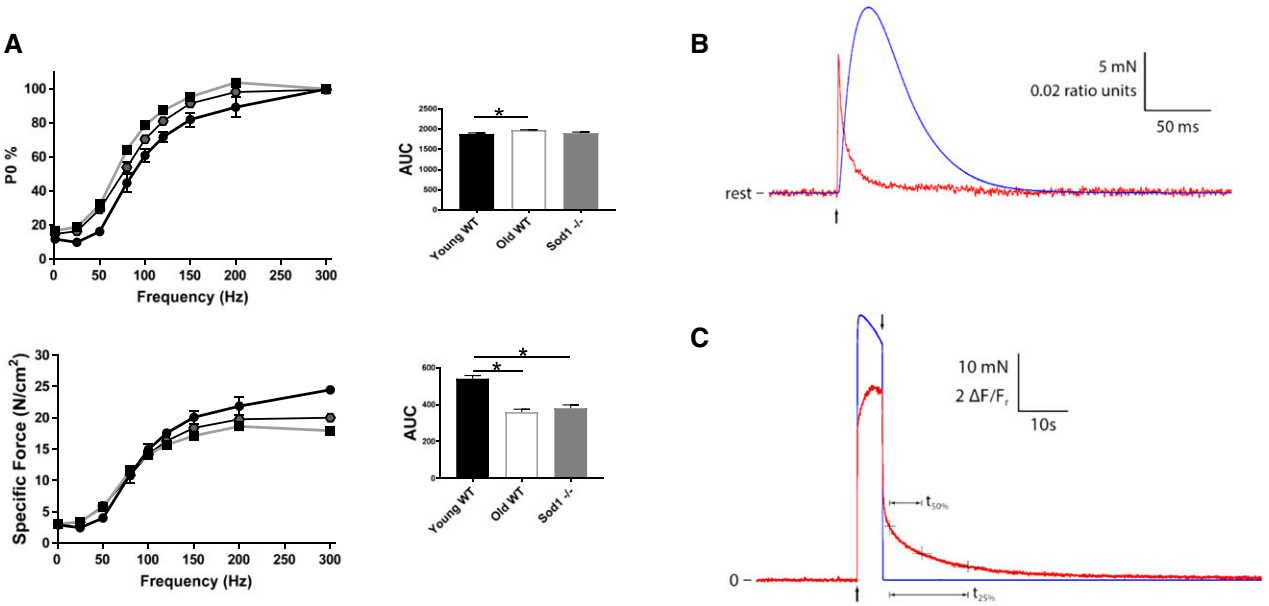

would show reduced SERCA pump activity in a manner similar to old WT mice. Measurement of SR Ca^{2+}-ATPase activity was determined by measuring the decrease in NADH absorbance at 340 nm in gastrocnemius homogenates from young WT, old WT, and *Sod1*$^{-/-}$ mice. The maximal rate of change in NADH absorbance was significantly reduced by ≈14% (P = 0.004) and ≈33% ($P < 0.001$) in the old WT and *Sod1*$^{-/-}$ mice, respectively, when compared with young WT (*Figure* 4A). The SERCA pump dysfunction cannot be explained by altered SERCA expression because WB analysis failed to detect any reduction in protein levels of SERCA1 and SERCA2 isoforms (*Figure* 4B). The protein expression of SERCA1, the most abundant SERCA isoform, was unchanged in the gastrocnemius muscles of the three groups, while SERCA2 expression was upregulated in *Sod1*$^{-/-}$ mice (≈57%, $P < 0.05$) when compared with young WT mice (*Figure* 4B).

Sarcolipin, a small membrane protein, inhibits SERCA by reducing the apparent Ca^{2+} affinity of the pump.[42] We hypothesized that an elevated level of sarcolipin could account for compromised SERCA function. Although we could not detect sarcolipin protein expression in the soleus and red gastrocnemius muscles of the young WT mice, we observed a high level of sarcolipin protein expression in muscle from old WT and *Sod1*$^{-/-}$ mice (*Figure* 4C). Similar changes were observed in mRNA expression in the old WT (almost equal to five-fold increase, P = 0.003) and the *Sod1*$^{-/-}$ mice (≈500-fold increase, P = 0.004) (*Figure* 4C). These results suggest that the sarcolipin may contribute to the impaired SERCA function in the old WT and the *Sod1*$^{-/-}$ mice. Indeed, the overexpression of sarcolipin is associated with reduced SERCA function and impaired muscle force in the rat soleus.[43]

Voltage sensors and sarcoplasmic reticulum calcium handling proteins

The reduction in SERCA pump activity and force-generating capacity implicate potential alterations in the quantity and/or quality of proteins involved in voltage sensing and calcium handling. To determine whether the deficiency of *Sod1* can affect these proteins in a manner similar to ageing phenotype, we measured the expression levels of proteins involved in voltage sensing and SR calcium handling in the gastrocnemius muscle of young WT, old WT, and *Sod1*$^{-/-}$ mice. We hypothesized that the expression of SR calcium binding and release units will be affected by the loss of

DOI: 10.1002/jcsm.12339

Figure 3 Intracellular calcium transients. Parameters of calcium release and sequestration in the intact lumbrical muscles from the young wild-type (WT) and *Sod1*$^{-/-}$ mice. Intracellular calcium transient (ICT) peak was reduced, while the ICT fall time and width durations were prolonged during the large, rapid calcium transients associated with twitch contractions in *Sod1*$^{-/-}$ compared with WT mice (A). No difference was detected between lumbrical muscles from *Sod1*$^{-/-}$ and WT mice in either the resting calcium level or the slow return to resting level following a long tetanic contraction (B). Values are expressed as mean ± SEM (n = 6–9 per group); one-way analysis of variance. $^{*}P \leq 0.05$, $^{**}P \leq 0.01$, $^{***}P \leq 0.001$.

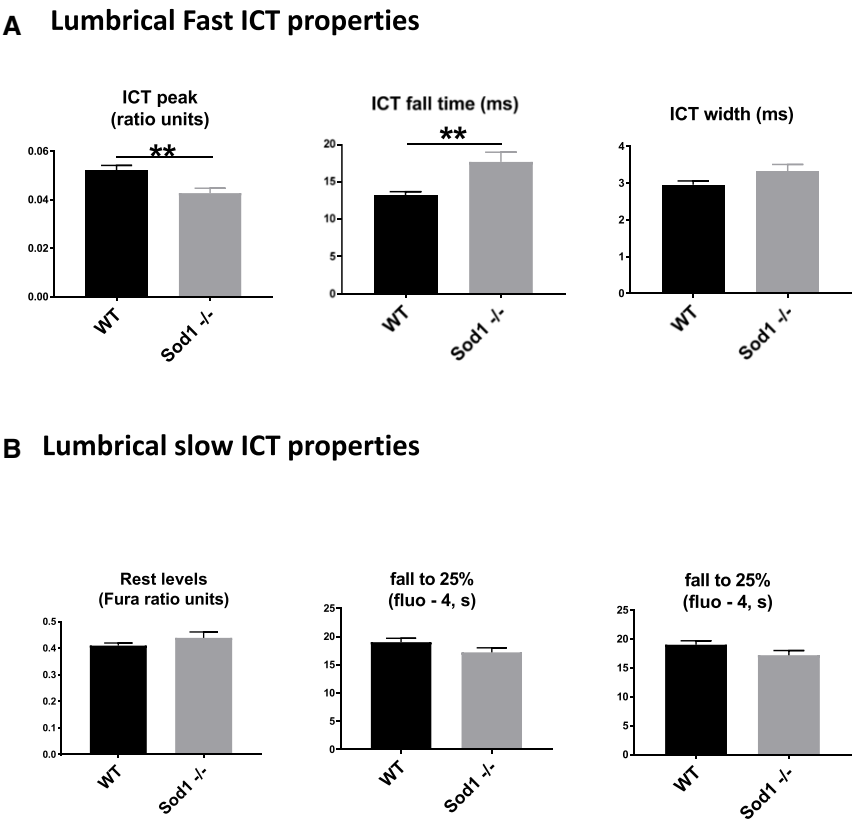

Sod1. As shown in *Figure* 5, there is a reduced expression of calstabin relative to RyR expression (≈21%, $P < 0.05$) in the *Sod1*$^{-/-}$ mice when compared with young WT mice. Calstabin is the major stabilizing unit of the calcium release channels, RyRs, and its dissociation and reduced relative expression from RyR have been implicated in impaired muscle quality.[44] There was no effect of age and *Sod1* deficiency on the RyR protein expression. Further, calsequestrin that binds Ca^{2+} in the SR lumen is increased in the old WT (≈45%, P = 0.009) but not in *Sod1*$^{-/-}$ mice (P = 0.902) when compared with young WT mice. The protein level of the voltage sensor α-1 subunit of the DHPR was upregulated in *Sod1*$^{-/-}$ mice (≈45%, $P < 0.05$), while α-2 subunit protein expression was unchanged.

Force-generating machinery and its regulators

Preferential loss of MHC, the major molecular motor of the myofibril, is shown to be associated with age-related muscle atrophy.[45] In accordance with this previous report, we found a selective loss of MHC in the gastrocnemius muscles of the old WT mice (≈14%, $P < 0.05$), which is recapitulated in the *Sod1*$^{-/-}$ mice (≈17%, $P < 0.05$) when compared with young WT mice (*Figure* 6A). Because the activation of calpain or calcium-dependent cysteine protease is the major contributor of sarcomeric myosin degradation,[46] we measured calpain activity. Cleavage of α-spectrin to signature fragment of 145 kDa correlates well with the calpain activity.[47] Accordingly, with the MHC loss, we observed an increased expression of calpain-specific breakdown product of α-spectrin in the gastrocnemius muscles of old WT (almost equal to six-fold, $P < 0.05$) and *Sod1*$^{-/-}$ mice (almost equal to nine-fold, $P < 0.05$) when compared with young WT mice (*Figure* 6A). We next assessed calpain activity in the muscle homogenates using fluorogenic substrate and found higher activity in the *Sod1*$^{-/-}$ mice (≈22%, $P < 0.01$) when compared with young WT mice although old WT mice did not show significant difference from young WT mice (*Figure* 6B). The calpain protein showed an increased level, albeit not statistically significant in the old WT (P = 0.446) and *Sod1*$^{-/-}$ mice (P = 0.431) when compared with young WT mice.

DOI: 10.1002/jcsm.12339

Figure 4 Sarcoplasmic reticulum Ca^{2+} ATPase (SERCA) pump activity and protein expression. (A) SERCA Ca^{2+}-dependent ATPase activity and the maximal ATPase activity (V_{max}) in gastrocnemius muscle homogenates; (B) western blot analysis of SERCA protein content; and (C) sarcolipin protein and mRNA expressions and phospholamban (PLB) mRNA expression from the gastrocnemius muscles of young and old wild-type (WT) and *Sod1*$^{-/-}$ mice. Values are expressed as mean ± SEM (n = 8–12 per group); one-way analysis of variance. $^{*}P \leq 0.05$, $^{**}P \leq 0.01$, $^{***}P \leq 0.001$. SLN, sarcolipin.

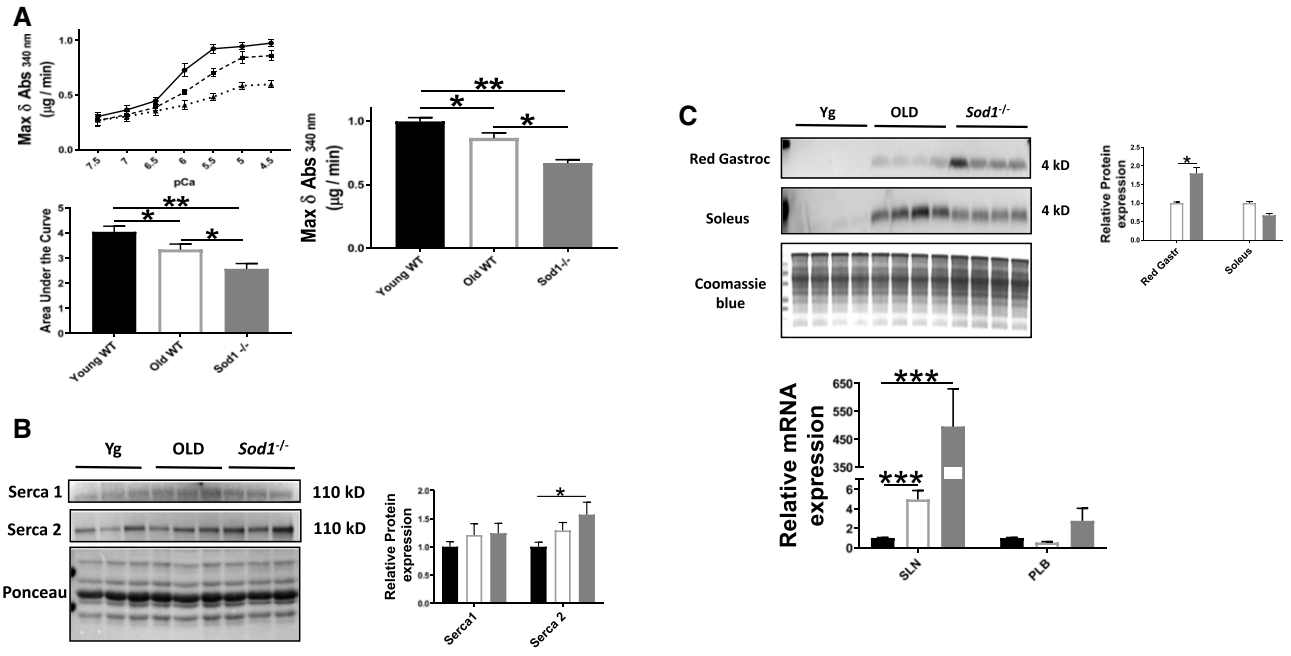

Figure 5 Expression of other EC coupling proteins. Western blot analysis of EC coupling protein content in gastrocnemius muscles of young and old wild-type and *Sod1*$^{-/-}$ mice. Values are expressed as mean ± SEM (n = 8–12 per group); one-way analysis of variance. $^{*}P \leq 0.05$, $^{**}P \leq 0.01$, $^{***}P \leq 0.001$. DHPR, dihydropyridine receptor; RyR, ryanodine receptor.

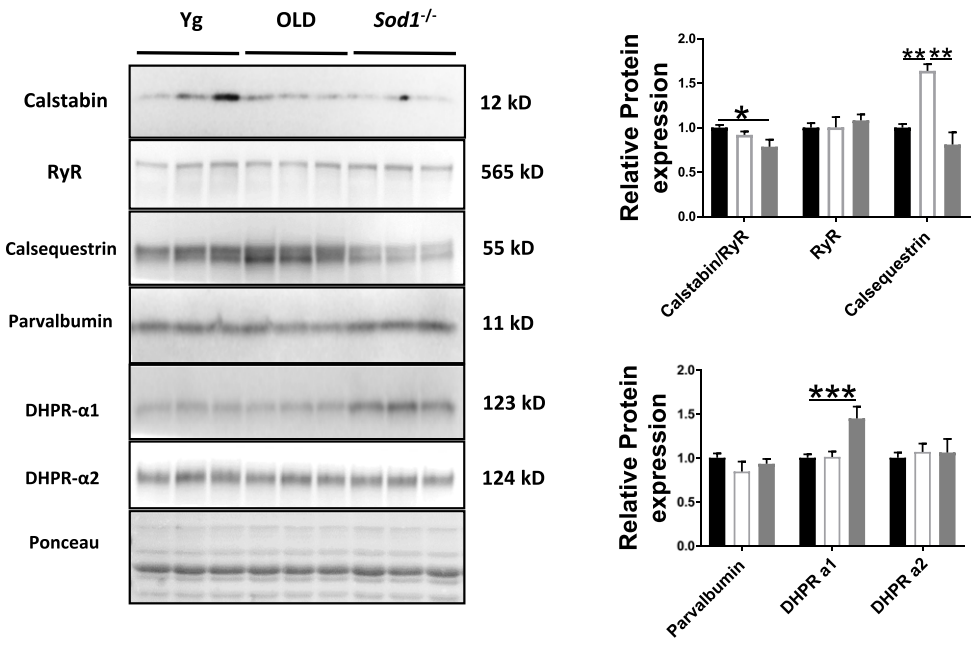

DOI: 10.1002/jcsm.12339

Figure 6 Myosin heavy chain (MHC) content and calpain protease activity. (A) MHC content normalized to total protein content; (B) western blot analysis of calpain content and α-2 spectrin cleavage as a measure of calpain activity; and (C) calpain activity as measured by cleavage of fluorogenic substrate in the gastrocnemius muscles of young and old wild-type and *Sod1*$^{-/-}$ mice. Values are expressed as mean ± SEM (n = 8–12 per group); one-way analysis of variance. $^{*}P \leq 0.05$, $^{**}P \leq 0.01$, $^{***}P \leq 0.001$.

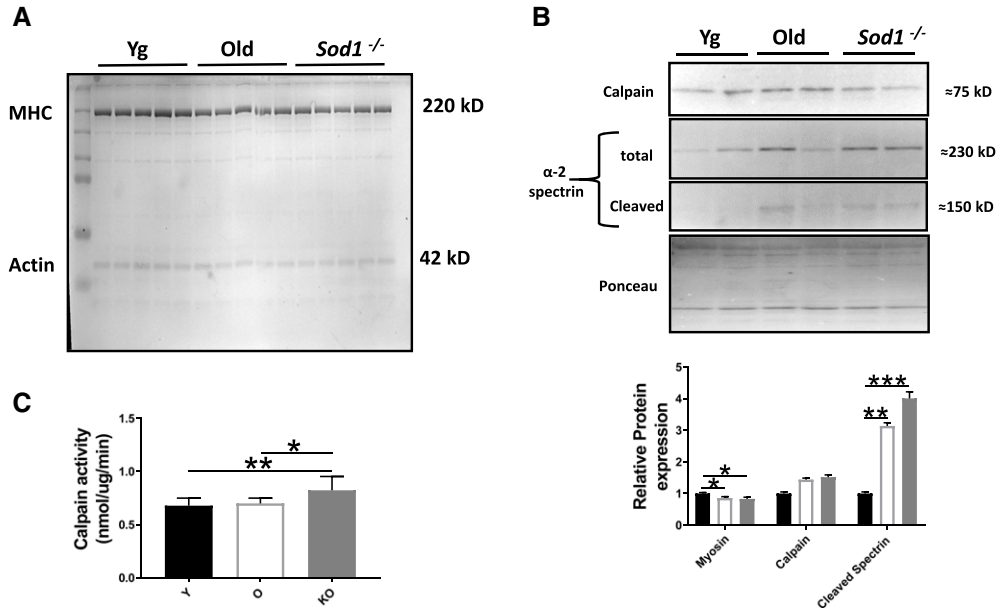

Figure 7 Markers of oxidative stress. (A) Protein carbonylation detected using avidin-fluorescein isothiocyanate (FITC) affinity staining in gastrocnemius muscle; (B) F_2-isoprostane levels in quadriceps muscle; and (C) western blot analysis of the nitrated proteins from the gastrocnemius muscles of young and old wild-type (WT) and *Sod1*$^{-/-}$ mice. Values are expressed as mean ± SEM (n = 8–12 per group); one-way analysis of variance. $^{*}P \leq 0.05$, $^{***}P \leq 0.001$, $^{****}P \leq 0.0001$.

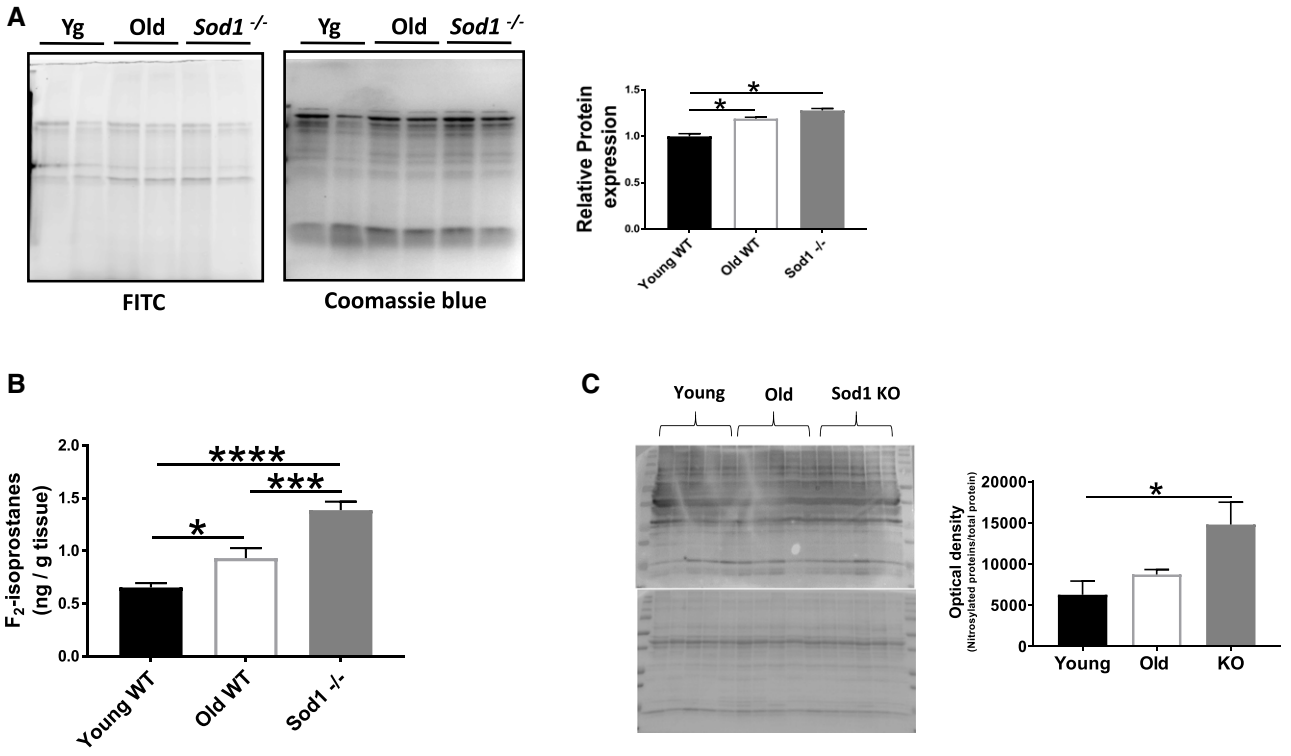

DOI: 10.1002/jcsm.12339

Post-translational modifications

We next assessed the markers of oxidative damage in the old WT and *Sod1*$^{-/-}$ mice. F_2-isoprostane and protein carbonyl levels were significantly higher in old WT mice (F_2-isoprostanes; ≈42%, $P < 0.05$, proteins carbonyls; ≈19%, $P < 0.05$) and in the *Sod1*$^{-/-}$ mice (F_2-isoprostanes; ≈112%, $P < 0.05$, protein carbonyls; ≈28%, $P < 0.05$), while protein S-nitrosylation was only increased in the *Sod1*$^{-/-}$ mice (≈136%, $P < 0.05$) when compared with young WT mice. Considering the vulnerability of EC coupling proteins to the oxidative damage,[48] we postulate that the oxidative stress is a significant contributor to the EC uncoupling in the old WT and *Sod1*$^{-/-}$ mice (*Figure* 7A to 7C).

Calcium signalling proteins

Cytosolic Ca^{2+} is an important contributor to skeletal muscle plasticity by activating specific signalling pathways. Accordingly, we looked at the protein expression of calmodulin/calcineurin and NFAT proteins. No significant difference was found in the old WT and *Sod1*$^{-/-}$ mice when compared with young WT mice (*Figure* 8A and 8B). NFAT proteins control muscle fibre-type distribution, which is also unchanged among the three experimental groups (*Figure* 8D). However, DSCR1, an inhibitor of calcineurin, was significantly elevated in the *Sod1*$^{-/-}$ mice when compared with young WT mice (*Figure* 8C). These findings, nevertheless, do not exclude changes in enzyme activities of these proteins.

Discussion

Ageing is associated with a decline in muscle force generation, which is explained by reduced muscle quantity and quality. Despite many reports of age-related loss of muscle quality, the mechanism(s) between oxidative stress and muscle quality remain to be elucidated. We have previously recapitulated many features of the ageing phenotype in our *Sod1*$^{-/-}$ mouse model of sarcopenia, including denervation, atrophy, and reduced muscle specific force.[38,49] The reduction in specific force is independent of muscle size and neuronal stimulation[49] and relates to a deficit in the intrinsic force-generating properties of the muscle. These findings prompted us to look at components of sarcolemmal excitation, SR calcium handling, and the muscle contraction. The results from this study support and extend the sarcopenia phenotype of *Sod1*$^{-/-}$ mice and more importantly provide clues to the underlying mechanisms of

Figure 8 Calcium signalling and muscle fibre-type composition. (A, B, and C) Western blot analysis of calcium signalling proteins levels and (D) muscle fibre-type composition and cross-sectional areas from the gastrocnemius muscles of young and old wild-type (WT) and *Sod1*$^{-/-}$ mice. Values are expressed as mean ± SEM (n = 8–12 per group); one-way analysis of variance. $^{*}P \leq 0.05$, $^{**}P \leq 0.01$. CSA, cross-sectional area; NFAT, nuclear factor of activated T-cells.

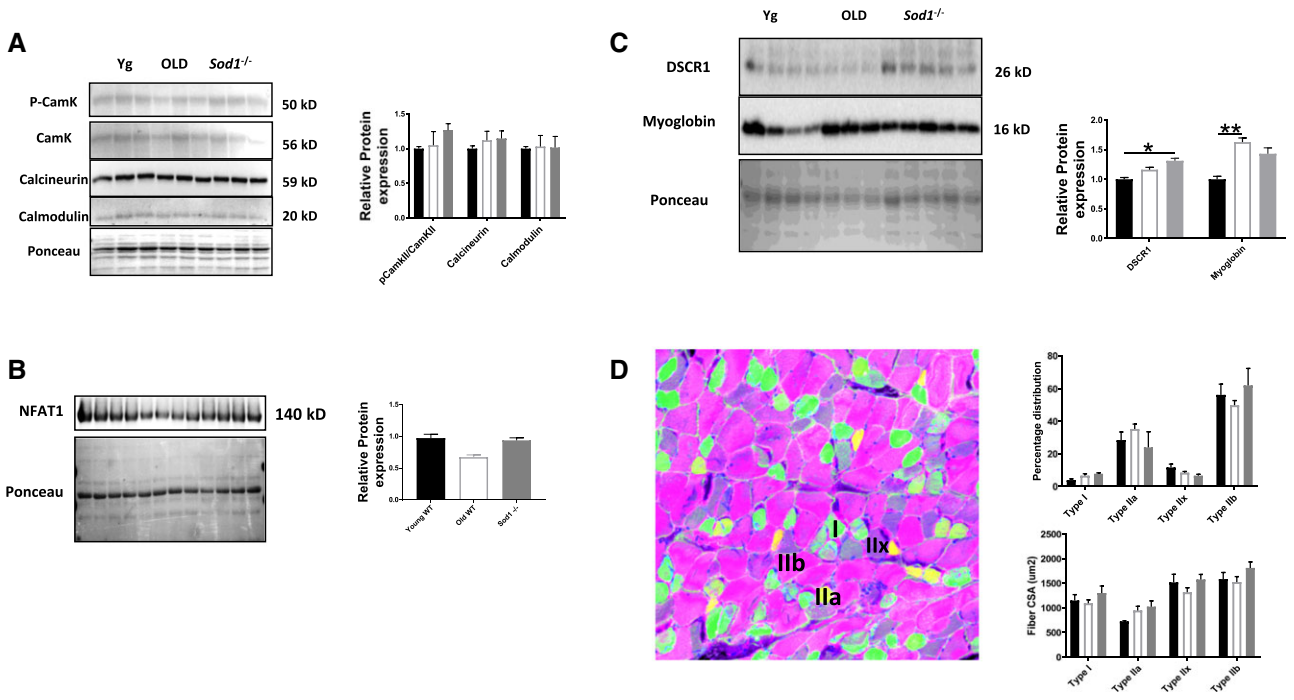

DOI: 10.1002/jcsm.12339

sarcopenia in humans. We report that the disruption of excitation–contraction coupling contributes to impaired force generation in the mouse model of *Sod1* deficiency. Briefly, we found a significant reduction in SERCA activity as well as reduced expression of proteins involved in calcium release and force generation. Another potential factor involved in EC uncoupling in *Sod1*$^{-/-}$ mice is oxidative damage to proteins involved in the contractile response. Here, we found an increase in markers of global protein carbonylation and nitration as well as markers of lipid peroxidation (F_2-isoprostanes). Together, the loss of quantity and quality of EC-coupling machinery in *Sod1*$^{-/-}$ mice is in agreement with impaired force generation we report in our study.

Intracellular calcium transients associated with twitch contractions reach high levels at their peak (≈20 μM) and undergo rapid changes throughout.[50] As such, only low-affinity calcium sensors such as mag-fura-2 are capable of reporting calcium responses to twitch stimulation without saturation or kinetic delay.[33] The time course of the twitch transient as reported by low-affinity dyes consists of a large, very rapid increase due to release of calcium from the SR followed by an equally large, less rapid fall to resting level. The fall in cytoplasmic calcium is due primarily to rapid binding to troponin and parvalbumin, with little contributing from the SR pump.[50,51] The finding that the peak of the twitch calcium transient was reduced by 20% in muscles from the *Sod1*$^{-/-}$ mice with no change in width or full duration of half maximum (FDHM) is similar to that reported in fibres from *mdx* mice.[52] Modelling simulations by those authors suggested that the result is consistent with a reduction in calcium release coupled with a reduced binding of calcium by parvalbumin, which could also contribute to the 35% slowing of fall time observed in the present study. A number of mechanisms including reduced RyR expression and/or its coupling with DHPR and calstabin can lead to reduced calcium release. However, we did not observe any significant reduction in the RyR expression in the two groups, which is consistent with previous findings in studies of ageing rodents.[53,54] The long half-life (5–8 days) of the RyR is further increased (≈25%) with ageing,[55] theoretically making it susceptible to post-translational modifications. Accordingly, oxidative damage to RyR can result in irreversible inactivation of the channel, leading to defective Ca^{2+} release and force generation.[53,56] The increased level of biomarkers of oxidative damage to both lipids and proteins is compatible with potential damage to the RyR resulting in muscle deficits. Further, the reduced relative expression of the RyR stabilizing unit, calstabin, observed in *Sod1*$^{-/-}$ mice can also contribute to reduced EC coupling and Ca^{2+} release in a manner similar to models of cardiac diseases[57] and overtraining.[44] In fact oxidative damage to calstabin has been linked to its dissociation and reduced relative expression to the RyR, resulting in calcium leak.[54] Muscle ageing can also result in changes in DHPR subunits and their coupling with the RyR leading to defective calcium release upon stimulation.[58] We only found significant increase in the α-2 subunit of the DHPR in the *Sod1*$^{-/-}$ mice, while the α-1 subunit was unchanged, but this observation, nevertheless, does not exclude physical dissociation between DHPR and RyR at the triad junction.

Calcium clearance from the sarcoplasm dictates $RT_{1/2}$ and is primarily regulated by SERCA pumps in the SR membrane. The significant reduction in SERCA pump activity of *Sod1*$^{-/-}$ mice mimics the reduction in conditions of increased oxidative stress such as ageing[59] and chronic diseases.[60] In adult skeletal muscle, two SERCA isoforms predominate, namely, SERCA1 and SERCA2, with the former being most abundant in fast-twitch mouse gastrocnemius muscle. However, our measures of SERCA protein content showed no change in SERCA1, while SERCA2 protein is significantly upregulated in the *Sod1*$^{-/-}$ mice. Hence, the mechanism(s) underlying reduced SERCA activity do not involve changes in SERCA pump expression. It is possible that post-translational modification(s) of SERCA could compromise its function. Like the RyR, SERCA has a long half-life of ≈14–17 days, making it potentially susceptible to oxidative damage.[55] Previous studies have demonstrated an age-related nitrosylation of SERCA proteins,[59] which is most prominent in SERCA2 proteins. Here, we report an increase in the global protein nitration in the *Sod1*$^{-/-}$ mice, which is consistent with the hypothesis that nitrosylation of SERCA may contribute to the reduced SERCA activity. Another possible mechanism underlying reduced SERCA activity is inhibition by sarcolipin, which is a SERCA pump inhibitor.[42] Upregulation of sarcolipin protein and/or mRNA expression has been associated with SERCA dysfunction, Ca^{2+} dysregulation, and myopathies.[61–63] Furthermore, studies in mouse models of muscular dystrophy suggest that its overexpression may be directly proportional to disease severity.[63] We found high expression of sarcolipin mRNA in the gastrocnemius muscles of old WT and *Sod1*$^{-/-}$ mice but not in young WT mice. These findings are mirrored at the protein level in the soleus and red gastrocnemius muscles. Sarcolipin overexpression has been shown to result in reduced SERCA activity and contractile impairment in rodent skeletal muscle.[43] Thus, it is probable that the increased expression of sarcolipin in aged and *Sod1*$^{-/-}$ mouse muscle contributes to the reduced SERCA activity in these models which in turn reduces the SR Ca^{2+} reserves, resulting in reduced Ca^{2+} release upon stimulation and subsequent muscle functional deficit.

Elevated oxidative stress may also induce EC uncoupling by affecting the SR calcium buffering proteins. Although *Sod1*$^{-/-}$ mice do not show any significant change in calsequestrin 1 and parvalbumin protein levels, we cannot exclude phosphorylation and/or oxidative damage to them in cellular redox environment.

The preferential loss of molecular motor protein MHC in the *Sod1*$^{-/-}$ mice recapitulates the age-related loss of

MHC as reported elsewhere.[45,64] This selective reduction of MHC may lead to a decrease in number of active cross bridges involved in force generation, contributing to muscle weakness. The selective reduction of MHC is not unprecedented and is previously reported in conditions of increased oxidative stress including muscle disease[65] and disuse.[66] Myosin and other cytoskeletal proteins are mainly cleaved by calpains, the calcium-activated cysteine proteases.[67] Accordingly, we report an increased calpain activation in *Sod1*$^{-/-}$ mice as assessed by an increase in calpain-dependent cleavage products of α-2 spectrin and fluorogenic substrate.

In summary, this study provides strong support for the coupling between increased oxidative stress and disruption of cellular excitation contraction machinery in mouse skeletal muscle. We report that the muscle weakness in the *Sod1*$^{-/-}$ mice is in part caused by reactive oxygen species-mediated EC uncoupling, which results in reduced quality and/or quantity of machinery involved in SR calcium handling and force generation. The novel quantitative mechanistic data provided here can lead to potential therapeutic interventions of SERCA dysfunction for sarcopenia and muscle diseases.

Acknowledgements

This work was supported by a P01 grant (AG051442) from NIA/NIH and Veterinary Affairs (VA) Merit Grant from the Department of Veterans Affairs to Dr. Van Remmen. Dr. Van Remmen is also supported by a Senior VA Research Career Scientist Award from the Department of Veterans Affairs. The authors certify that they comply with ethical guidelines for authorship and publishing of the Journal of Cachexia, Sarcopenia and Muscle.[68]

Online supplementary material

Additional supporting information may be found online in the Supporting Information section at the end of the article.

Figure S1. Muscle fatigue. Time course of contractile force decline in EDL muscles during 400 seconds of fatiguing stimulations. Values are expressed as Mean ± SEM (n = 8–12 per group).; One-way ANOVA. * $P \leq 0.05$, ** $P \leq 0.01$, *** $P \leq 0.001$, **** $P \leq 0.0001$ ANOVA.

Figure S2. Expressions of genes associated with muscle quantity and quality. mRNA expression of genes associated with muscle functional and structural phenotypes in the gastrocnemius muscles of young and old WT and Sod 1 $^{-/-}$ mice. Values are expressed as Mean ± SEM (n = 8–12 per group). One-way ANOVA. * $P \leq 0.05$.

Conflict of interest

Rizwan Qaisar, Shylesh Bhaskaran, Pavithra Premkumar, Rojina Ranjit, Kavithalakshmi Satara Natarajan, Bumsoo Ahn, Kaitlyn Riddle, Dennis R Claflin, Arlan Richardson, Susan V. Brooks, and Holly Van Remmen declare they have no conflict of interest.

References

1. Ali S, Garcia JM. Sarcopenia, cachexia and aging: diagnosis, mechanisms and therapeutic options—a mini-review. *Gerontology* 2014;**60**:294–305.
2. Larsson L, Li X, Yu F, Degens H. Age-related changes in contractile properties and expression of myosin isoforms in single skeletal muscle cells. *Muscle Nerve Suppl* 1997;**5**:S74–S78.
3. Mitchell WK, Williams J, Atherton P, Larvin M, Lund J, Narici M. Sarcopenia, dynapenia, and the impact of advancing age on human skeletal muscle size and strength; a quantitative review. *Front Physiol* 2012;**3**:260.
4. Delbono O. Expression and regulation of excitation-contraction coupling proteins in aging skeletal muscle. *Curr Aging Sci* 2011;**4**:248–259.
5. Muller FL, Song W, Jang YC, Liu Y, Sabia M, Richardson A, Van Remmen H. Denervation-induced skeletal muscle atrophy is associated with increased mitochondrial ROS production. *Am J Physiol Regul Integr Comp Physiol* 2007;**293**:R1159–R1168.
6. Baylor SM, Hollingworth S. Intracellular calcium movements during excitation-contraction coupling in mammalian slow-twitch and fast-twitch muscle fibers. *J Gen Physiol* 2012;**139**:261–272.
7. Lee CS, Dagnino-Acosta A, Yarotskyy V, Hanna A, Lyfenko A, Knoblauch M, Georgiou DK, Poché RA, Swank MW, Long C, Ismailov II, Lanner J, Tran T, Dong K, Rodney GG, Dickinson ME, Beeton C, Zhang P, Dirksen RT, Hamilton SL. Ca(2+) permeation and/or binding to CaV1.1 fine-tunes skeletal muscle Ca(2+) signaling to sustain muscle function. *Skelet Muscle* 2015;**5**:4.
8. Cheng AJ, Yamada T, Rassier DE, Andersson DC, Westerblad H, Lanner JT. Reactive oxygen/nitrogen species and contractile function in skeletal muscle during fatigue and recovery. *J Physiol* 2016;**594**:5149–5160.
9. Viner RI, Ferrington DA, Williams TD, Bigelow DJ, Schöneich C. Protein modification during biological aging: selective tyrosine nitration of the SERCA2a isoform of the sarcoplasmic reticulum Ca2+-ATPase in skeletal muscle. *Biochem J* 1999;**340**:657–669.
10. Delbono O. Molecular mechanisms and therapeutics of the deficit in specific force in ageing skeletal muscle. *Biogerontology* 2002;**3**:265–270.
11. Plant DR, Lynch GS. Excitation-contraction coupling and sarcoplasmic reticulum function in mechanically skinned fibres from fast skeletal muscles of aged mice. *J Physiol* 2002;**543**:169–176.
12. Ingalls CP, Warren GL, Williams JH, Ward CW, Armstrong RB. EC coupling failure in

mouse EDL muscle after in vivo eccentric contractions. *J Appl Physiol (1985)* 1998;**85**:58–67.
13. Manring H, Abreu E, Brotto L, Weisleder N, Brotto M. Novel excitation-contraction coupling related genes reveal aspects of muscle weakness beyond atrophy-new hopes for treatment of musculoskeletal diseases. *Front Physiol* 2014;**5**:37.
14. Jackson MJ. Lack of CuZnSOD activity: a pointer to the mechanisms underlying age-related loss of muscle function, a commentary on "absence of CuZn superoxide dismutase leads to elevated oxidative stress and acceleration of age-dependent skeletal muscle atrophy". *Free Radic Biol Med* 2006;**40**:1900–1902.
15. Larkin LM, Davis CS, Sims-Robinson C, Kostrominova TY, Van Remmen H, Richardson A, Feldman EL, Brooks SV. Skeletal muscle weakness due to deficiency of CuZn-superoxide dismutase is associated with loss of functional innervation. *Am J Physiol Regul Integr Comp Physiol* 2011; **301**:R1400–R1407.
16. Ivannikov MV, Van Remmen H. Sod1 gene ablation in adult mice leads to physiological changes at the neuromuscular junction similar to changes that occur in old wild-type mice. *Free Radic Biol Med* 2015;**84**:254–262.
17. Larkin LM, Hanes MC, Kayupov E, Claflin DR, Faulkner JA, Brooks SV. Weakness of whole muscles in mice deficient in Cu, Zn superoxide dismutase is not explained by defects at the level of the contractile apparatus. *Age (Dordr)* 2013;**35**:1173–1181.
18. Delbono O. Calcium current activation and charge movement in denervated mammalian skeletal muscle fibres. *J Physiol* 1992;**451**:187–203.
19. Ray A, Kyselovic J, Leddy JJ, Wigle JT, Jasmin BJ, Tuana BS. Regulation of dihydropyridine and ryanodine receptor gene expression in skeletal muscle. Role of nerve, protein kinase C, and cAMP pathways. *J Biol Chem* 1995;**270**:25837–25844.
20. Kern H, Boncompagni S, Rossini K, Mayr W, Fanò G, Zanin ME, Podhorska-Okolow M, Protasi F, Carraro U. Long-term denervation in humans causes degeneration of both contractile and excitation-contraction coupling apparatus, which is reversible by functional electrical stimulation (FES): a role for myofiber regeneration? *J Neuropathol Exp Neurol* 2004;**63**:919–931.
21. Sakellariou GK, Pye D, Vasilaki A, Zibrik L, Palomero J, Kabayo T, McArdle F, Van Remmen H, Richardson A, Tidball JG, McArdle A, Jackson MJ. Role of superoxide-nitric oxide interactions in the accelerated age-related loss of muscle mass in mice lacking Cu,Zn superoxide dismutase. *Aging Cell* 2011;**10**:749–760.
22. Smith IC, Vigna C, Levy AS, Denniss SG, Rush JW, Tupling AR. The effects of buthionine sulfoximine treatment on diaphragm contractility and SERCA pump function in adult and middle aged rats. *Physiol Rep* 2015;**3**:e12547.
23. Elchuri S, Oberley TD, Qi W, Eisenstein RS, Jackson Roberts L, Van Remmen H, Epstein CJ, Huang TT. CuZnSOD deficiency leads to persistent and widespread oxidative damage and hepatocarcinogenesis later in life. *Oncogene* 2005;**24**:367–380.
24. Zhang Y, Ikeno Y, Bokov A, Gelfond J, Jaramillo C, Zhang H-M, Liu Y, Qi W, Hubbard G, Richardson A, Van Remmen H. Dietary restriction attenuates the accelerated aging phenotype of Sod1(−/−) mice. *Free Radic Biol Med* 2013; **60**:300–306.
25. Roberts BM, Frye GS, Ahn B, Ferreira LF, Judge AR. Cancer cachexia decreases specific force and accelerates fatigue in limb muscle. *Biochem Biophys Res Commun* 2013;**435**:488–492.
26. Claflin DR, Brooks SV. Direct observation of failing fibers in muscles of dystrophic mice provides mechanistic insight into muscular dystrophy. *Am J Physiol Cell Physiol* 2008;**294**:C651–C658.
27. Fu MH, Tupling AR. Protective effects of Hsp70 on the structure and function of SERCA2a expressed in HEK-293 cells during heat stress. *Am J Physiol Heart Circ Physiol* 2009;**296**:H1175–H1183.
28. Supinski GS, Wang W, Callahan LA. Caspase and calpain activation both contribute to sepsis-induced diaphragmatic weakness. *J Appl Physiol* 1985), 2009;**107**:1389–1396.
29. Brachmanski M, Gebhard MM, Nobiling R. Separation of fluorescence signals from Ca2+ and NADH during cardioplegic arrest and cardiac ischemia. *Cell Calcium* 2004;**35**:381–391.
30. Jobsis FF, Stainsby WN. Oxidation of NADH during contractions of circulated mammalian skeletal muscle. *Respir Physiol* 1968; **4**:292–300.
31. Claflin DR, Jackson MJ, Brooks SV. Age affects the contraction-induced mitochondrial redox response in skeletal muscle. *Front Physiol* 2015;**6**:21.
32. Gee KR, Brown KA, Chen WN, Bishop-Stewart J, Gray D, Johnson I. Chemical and physiological characterization of fluo-4 Ca(2+)-indicator dyes. *Cell Calcium* 2000;**27**:97–106.
33. Konishi M, Hollingworth S, Harkins AB, Baylor SM. Myoplasmic calcium transients in intact frog skeletal muscle fibers monitored with the fluorescent indicator furaptra. *J Gen Physiol* 1991;**97**:271–301.
34. Ahn B, Rhee SG, Stadtman ER. Use of fluorescein hydrazide and fluorescein thiosemicarbazide reagents for the fluorometric determination of protein carbonyl groups and for the detection of oxidized protein on polyacrylamide gels. *Anal Biochem* 1987;**161**:245–257.
35. Dyar KA, Ciciliot S, Wright LE, Biensø RS, Tagliazucchi GM, Patel VR, Forcato M, Paz MI, Gudiksen A, Solagna F, Albiero M, Moretti I, Eckel-Mahan KL, Baldi P, Sassone-Corsi P, Rizzuto R, Bicciato S, Pilegaard H, Blaauw B, Schiaffino S. Muscle insulin sensitivity and glucose metabolism are controlled by the intrinsic muscle clock. *Mol Metab* 2014;**3**:29–41.
36. Muller FL, Song W, Liu Y, Chaudhuri A, Pieke-Dahl S, Strong R, Huang TT, Epstein CJ, Roberts LJ 2nd, Csete M, Faulkner JA, Van Remmen H. Absence of CuZn superoxide dismutase leads to elevated oxidative stress and acceleration of age-dependent skeletal muscle atrophy. *Free Radic Biol Med* 2006;**40**:1993–2004.
37. Vasilaki A, van der Meulen JH, Larkin L, Harrison DC, Pearson T, Van Remmen H, Richardson A, Brooks SV, Jackson MJ, McArdle A. The age-related failure of adaptive responses to contractile activity in skeletal muscle is mimicked in young mice by deletion of Cu,Zn superoxide dismutase. *Aging Cell* 2010;**9**:979–990.
38. Shi Y, Ivannikov MV, Walsh ME, Liu Y, Zhang Y, Jaramillo CA, Macleod GT, Van Remmen H. The lack of CuZnSOD leads to impaired neurotransmitter release, neuromuscular junction destabilization and reduced muscle strength in mice. *PLoS One* 2014;**9**:e100834.
39. Jang YC, Liu Y, Hayworth CR, Bhattacharya A, Lustgarten MS, Muller FL, Chaudhuri A, Qi W, Li Y, Huang JY, Verdin E, Richardson A, Van Remmen H. Dietary restriction attenuates age-associated muscle atrophy by lowering oxidative stress in mice even in complete absence of CuZnSOD. *Aging Cell* 2012;**11**:770–782.
40. Viner RI, Ferrington DA, Aced GI, Miller-Schlyer M, Bigelow DJ, Schöneich C. In vivo aging of rat skeletal muscle sarcoplasmic reticulum Ca-ATPase. Chemical analysis and quantitative simulation by exposure to low levels of peroxyl radicals. *Biochim Biophys Acta* 1997;**1329**:321–335.
41. Green HJ, Burnett M, Duhamel TA, D'Arsigny C, O'Donnell DE, Webb KA, Ouyang J. Abnormal sarcoplasmic reticulum Ca2+-sequestering properties in skeletal muscle in chronic obstructive pulmonary disease. *Am J Physiol Cell Physiol* 2008;**295**:C350–C357.
42. Espinoza-Fonseca LM, Autry JM, Thomas DD. Sarcolipin and phospholamban inhibit the calcium pump by populating a similar metal ion-free intermediate state. *Biochem Biophys Res Commun* 2015;**463**:37–41.
43. Tupling AR, Asahi M, MacLennan DH. Sarcolipin overexpression in rat slow twitch muscle inhibits sarcoplasmic reticulum Ca2+ uptake and impairs contractile function. *J Biol Chem* 2002;**277**:44740–44746.
44. Bellinger AM, Reiken S, Dura M, Murphy PW, Deng SX, Landry DW, Nieman D, Lehnart SE, Samaru M, LaCampagne A, Marks AR. Remodeling of ryanodine receptor complex causes "leaky" channels: a molecular mechanism for decreased exercise capacity. *Proc Natl Acad Sci U S A* 2008;**105**:2198–2202.
45. Thompson LV, Durand D, Fugere NA, Ferrington DA. Myosin and actin expression and oxidation in aging muscle. *J Appl Physiol (1985)* 2006;**101**:1581–1587.
46. Smith IJ, Lecker SH, Hasselgren PO. Calpain activity and muscle wasting in sepsis. *Am J Physiol Endocrinol Metab* 2008;**295**: E762–E771.

47. Childers MK, Bogan JR, Bogan DJ, Greiner H, Holder M, Grange RW, Kornegay JN. Chronic administration of a leupeptin-derived calpain inhibitor fails to ameliorate severe muscle pathology in a canine model of duchenne muscular dystrophy. *Front Pharmacol* 2011;**2**:89.
48. van der Poel C, Edwards JN, Macdonald WA, Stephenson DG. Effect of temperature-induced reactive oxygen species production on excitation-contraction coupling in mammalian skeletal muscle. *Clin Exp Pharmacol Physiol* 2008;**35**: 1482–1487.
49. Jang YC, Lustgarten MS, Liu Y, Muller FL, Bhattacharya A, Liang H, Salmon AB, Brooks SV, Larkin L, Hayworth CR, Richardson A, Van Remmen H. Increased superoxide in vivo accelerates age-associated muscle atrophy through mitochondrial dysfunction and neuromuscular junction degeneration. *FASEB J* 2010;**24**:1376–1390.
50. Baylor SM, Hollingworth S. Simulation of Ca2+ movements within the sarcomere of fast-twitch mouse fibers stimulated by action potentials. *J Gen Physiol* 2007;**130**:283–302.
51. Hou TT, Johnson JD, Rall JA. Role of parvalbumin in relaxation of frog skeletal muscle. *Adv Exp Med Biol* 1993; **332**:141–151, discussion 151-3.
52. Hollingworth S, Zeiger U, Baylor SM. Comparison of the myoplasmic calcium transient elicited by an action potential in intact fibres of mdx and normal mice. *J Physiol* 2008;**586**:5063–5075.
53. Thomas MM, Vigna C, Betik AC, Tupling AR, Hepple RT. Initiating treadmill training in late middle age offers modest adaptations in Ca2+ handling but enhances oxidative damage in senescent rat skeletal muscle. *Am J Physiol Regul Integr Comp Physiol* 2010;**298**:R1269–R1278.
54. Russ DW, Grandy JS, Toma K, Ward CW. Ageing, but not yet senescent, rats exhibit reduced muscle quality and sarcoplasmic reticulum function. *Acta Physiol (Oxf)* 2011;**201**:391–403.
55. Ferrington DA, Krainev AG, Bigelow DJ. Altered turnover of calcium regulatory proteins of the sarcoplasmic reticulum in aged skeletal muscle. *J Biol Chem* 1998; **273**:5885–5891.
56. Sun J, Xu L, Eu JP, Stamler JS, Meissner G. Classes of thiols that influence the activity of the skeletal muscle calcium release channel. *J Biol Chem* 2001;**276**: 15625–15630.
57. Ward CW, Reiken S, Marks AR, Marty I, Vassort G, Lacampagne A. Defects in ryanodine receptor calcium release in skeletal muscle from post-myocardial infarct rats. *FASEB J* 2003;**17**:1517–1519.
58. Payne AM, Delbono O. Neurogenesis of excitation-contraction uncoupling in aging skeletal muscle. *Exerc Sport Sci Rev* 2004;**32**:36–40.
59. Schertzer JD, Plant DR, Ryall JG, Beitzel F, Stupka N, Lynch GS. Beta2-agonist administration increases sarcoplasmic reticulum Ca2+-ATPase activity in aged rat skeletal muscle. *Am J Physiol Endocrinol Metab* 2005;**288**:E526–E533.
60. Argiles JM, Fontes-Oliveira CC, Toledo M, López-Soriano FJ, Busquets S. Cachexia: a problem of energetic inefficiency. *J Cachexia Sarcopenia Muscle* 2014;**5**: 279–286.
61. Calvo AC, Manzano R, Atencia-Cibreiro G, Oliván S, Muñoz MJ, Zaragoza P, Cordero-Vázquez P, Esteban-Pérez J, García-Redondo A, Osta R. Genetic biomarkers for ALS disease in transgenic SOD1 (G93A) mice. *PLoS One* 2012;**7**:e32632.
62. Liu N, Bezprozvannaya S, Shelton JM, Frisard MI, Hulver MW, McMillan RP, Wu Y, Voelker KA, Grange RW, Richardson JA, Bassel-Duby R, Olson EN. Mice lacking microRNA 133a develop dynamin 2-dependent centronuclear myopathy. *J Clin Invest* 2011;**121**: 3258–3268.
63. Schneider JS, Shanmugam M, Gonzalez JP, Lopez H, Gordan R, Fraidenraich D, Babu GJ. Increased sarcolipin expression and decreased sarco (endo) plasmic reticulum Ca2+ uptake in skeletal muscles of mouse models of Duchenne muscular dystrophy. *J Muscle Res Cell Motil* 2013;**34**:349–356.
64. D'Antona G, Pellegrino MA, Adami R, Rossi R, Carlizzi CN, Canepari M, Saltin B, Bottinelli R. The effect of ageing and immobilization on structure and function of human skeletal muscle fibres. *J Physiol* 2003;**552**:499–511.
65. Haycock JW, Mac Neil S, Mantle D. Differential protein oxidation in Duchenne and Becker muscular dystrophy. *Neuroreport* 1998;**9**:2201–2207.
66. Ochala J, Gustafson AM, Diez ML, Renaud G, Li M, Aare S, Qaisar R, Banduseela VC, Hedström Y, Tang X, Dworkin B, Ford GC, Nair KS, Perera S, Gautel M, Larsson L. Preferential skeletal muscle myosin loss in response to mechanical silencing in a novel rat intensive care unit model: underlying mechanisms. *J Physiol* 2011; **589**:2007–2026.
67. Zhu X, van Hees HWH, Heunks L, Wang F, Shao L, Huang J, Shi L, Shaolin MA. The role of calpains in ventilator-induced diaphragm atrophy. *Intensive Care Med Exp* 2017;**5**:14.
68. von Haehling S, Morley JE, Coats AJS, Anker SD. Ethical guidelines for publishing in the Journal of Cachexia, Sarcopenia and Muscle: update 2017. *J Cachexia Sarcopenia Muscle* 2017;**8**:1081–1083.